Correspondence

PSK and DPSK Trellis Codes for Fast Fading, Shadowed Mobile Satellite Communication Channels

P. J. MCLANE, P. H. WITTKE, P. K.-M. HO, AND C. LOO

Abstract—**The performance of 8-PSK and 8-DPSK trellis codes is presented for a class of fast fading, land mobile satellite communication channels. As presented in the literature, the fading model is Rician but, in addition, the line-of-sight path is subjected to a fast lognormal attenuation that represents tree shadowing. The fading parameters used in this study represent the degree of shadowing and are based on measured data. The primary application considered here is for digital speech transmission and thus, bit error probabilities in the order of 10^{-3} are emphasized. Sensitivity of the bit error probability to amplitude fading, amplitude and phase fading, and decoding delay is presented. Performance is determined via digital computer simulation. Optimal four- and eight-state codes are determined and optimality is found to be dependent on the presence of lognormal shadowing.**

I. Introduction

This paper reports on the usefulness of rate 2/3, trellis coded, 8 phase-shift-keyed (8 PSK) and differential 8 PSK (8 DPSK) modulations for a class of land mobile satellite communications channels. Earlier, Divsalar and Simon [1] have presented results for trellis coded 8 PSK modulation for a Rician fading model without shadowing. The fading model used herein is documented in [2]–[5] where the line-of-sight (LOS) component of the Rician model is subjected to a lognormal transformation. This transformation represents the effect of foliage attenuation or blockage, also referred to as shadowing. The parameters for our model are based on measured data [2]–[5]. The model was developed for application in the Canadian Mobile Satellite Communications (MSAT) Program. Shadowing is more severe in Canada than in the United States due to a lower angle of elevation (15°–20°) between a mobile user and a suitably located geosynchonous satellite.

Trellis coded modulation was developed by Ungerboeck [6] for the additive white Gaussian noise (AWGN) channel. References [1], [7], [8], [9] represent their application to fading channels. The earlier references [10], [11] applied traditional bandwidth expanding, convolutional codes to the Rician channel for both PSK and DPSK modulations. Our results are based on a digital computer simulation of transmission over a shadowed Rician channel. Although a theory for the results we present would be well received, digital computer simulation will allow us to vary a number of system parameters and determine the resulting system performance. For instance, we find decision depths for Viterbi decoders can be smaller on fading channels than on the AWGN channel. In time delay constrained systems, like satellite communication systems, this allows greater interleaving depths to combat slow fades. As in [10], [11], a single sample per symbol interval is used to represent the signal fading process. Our interest is in vocoder generated speech transmission at a bit rate of 2400 bits/s and a bit error rate of 10^{-3}. The uncoded modulation is 4 PSK with a symbol rate of 1200 symbols/s. Most of our results are discussed in terms of this application. However, our results are presented in terms of unfaded signal-to-noise ratio and a fading bandwidth, normalized with respect to the symbol rate.

II. Transmission Model

We shall use a single sample per symbol to represent the transmission process. The channel is the additive white Gaussian noise channel with a time varying fading process representing the complex signal gain and this channel is illustrated in Fig. 1. The model is described by the following equations and we use phasor notation for each sample:

$$\boldsymbol{R}_i = \mathcal{L}[\{\boldsymbol{A}_i\}]e^{j\phi_i} + \boldsymbol{N}_i \quad (1)$$

$$\boldsymbol{A}_i = \boldsymbol{Z}_i + \boldsymbol{N}_{s,i} \quad (2)$$

where $\boldsymbol{R}_i$ is the received phasor, ϕ_i is the modulation phase (4 PSK or 8 PSK), $\boldsymbol{N}_i$ is the additive channel noise phasor with zero mean and variance $No/2$ W. $\boldsymbol{A}_i$ is the complex channel gain, $\{\boldsymbol{A}_i\} = (\boldsymbol{A}_i, \boldsymbol{A}_{i-1}, \cdots)$, and $\mathcal{L}[\{\boldsymbol{A}_i\}]$ is the effect of a linear, digital filter on $\boldsymbol{A}_i$. The linear filter is used to model the dynamics of the fading process. In (2), $Z_i = e^{n_i}$ where n_i is Gaussian with mean μ_o and variance d_o, is a lognormal random variable representing the effect of shadowing in the fading model. Also the scattering component of $\boldsymbol{A}_i$ is $\boldsymbol{N}_{s,i} = n_{ci} + jn_{si}$ where n_{ci} and n_{si} are Gaussian, with zero mean and variance b_o, and are mutually independent. The complex gain $\boldsymbol{A}_i$ is composed of the LOS component Z_i plus a scattering component, $\boldsymbol{N}_{si}$. In our model

$$\mathcal{L}[\{\boldsymbol{A}_i\}] = \mathcal{L}_1[\{Z_i\}] + \mathcal{L}_2[\{n_{ci}\}] + \mathcal{L}_3[\{n_{si}\}] \quad (3)$$

where $\mathcal{L}_i$, $i = 1, 3$ represents the effect of independent, third order, Butterworth filters of *the same 3 dB bandwidth B*. We used a third-order filter because it gave a good fit to experimental data for the shadowed Rician model from [2]–[5]. The normalized fading bandwidth is BT where T^{-1} is the symbol rate. The model parameters are from [2]–[5] and are given in Table I. Three cases are listed: light, average, and heavy shadowing, which represent an increasing effect of the lognormal process or the degree of shadowing. All parameters are normalized to a signal amplitude of unity. We have found that the light shadowing model has an envelope distribution that can be approximated by a Rician model (without shadowing) with a K factor between 4 and 6 dB. The K factor is the ratio of the power in the LOS component to the power in the scattered component of the Rician fading process. In this approximation, different K factors are needed for different sections of the amplitude distribution of the shadowed Rician

Paper approved by the Editor for Mobile Communications of the IEEE Communications Society. Manuscript received July 7, 1987; revised November 20, 1987. This work was supported by the Communications Research Centre, Department of Communications, Ottawa, Ont., Canada, under DSS Contract OST85-00197, and by the Natural Sciences and Engineering Research Council of Canada. This paper was presented at the 1987 International Conference on Communications, Seattle, WA, June 1987.

P. J. McLane and P. H. Wittke are with the Department of Electrical Engineering, Queen's University, Kingston, Ont., K7L 3N6, Canada.

P. K.-M. Ho is with the Department of Engineering Science, Simon Fraser University, Burnaby, BC, Canada.

C. Loo is with Communications Research Centre, Ottawa, Ont., Canada.

IEEE Log Number 8823630.

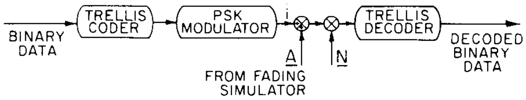

Fig. 1. Baseband signal transmission model.

TABLE I
SYSTEM PARAMETERS

	"Degree of Shadowing"		
	LIGHT	AVERAGE	HEAVY
b_0	0.158	0.126	0.0631
μ_0	0.115	-0.115	-3.91
$\sqrt{d_0}$	0.115	0.161	0.806

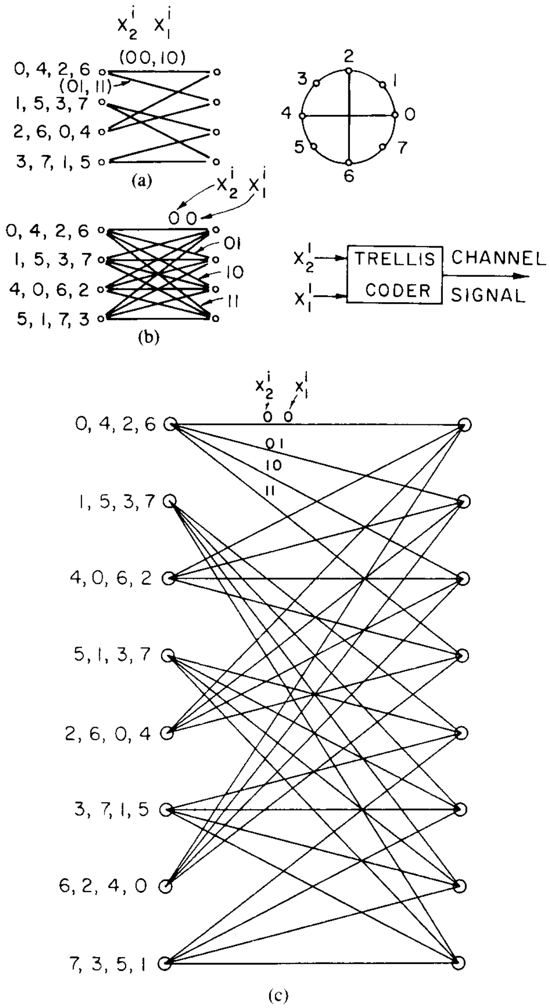

Fig. 2. (a) Ungerboeck's four-state, 8 PSK code, i.e., with parallel transitions. (b) The four-state, 8 PSK code without parallel transitions. (c) Ungerboeck's eight-state, 8 PSK code. The input bits, (x_2^i, x_1^i), which cause a particular state transition are labeled on the branch representing this state transition.

process. Thus, the shadowed Rician fading process is not equivalent to a Rician process.

The modulation phase considered herein is Gray coded for 4 PSK and trellis coded for 8 PSK or 8 DPSK. The trellis diagrams for the four- and eight-state codes to be considered are shown in Fig. 2. One four-state coder contains parallel

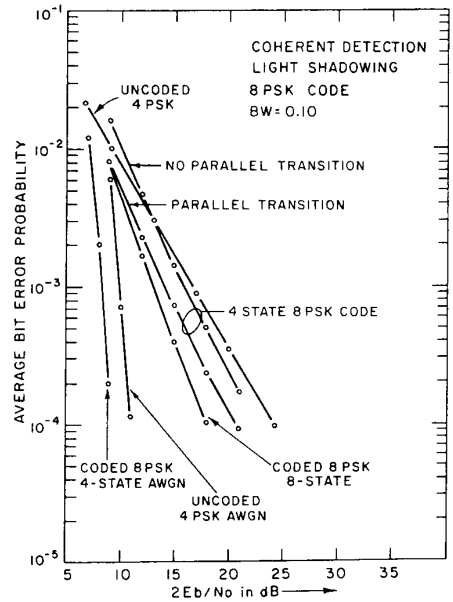

Fig. 3. Average bit error probability for the codes from Fig. 2 for a (normalized) fading bandwidth of 0.10 and a light shadowing fading model.

transitions, the other does not. Parallel transitions are optimum for the AWGN channel [6]. For the Rayleigh fading channel with infinite interleaving [12] shows that at high E_b/N_o the code in Fig. 2 without parallel transitions has a better bit error rate performance than the code with parallel transitions. The reason for this is that the code without parallel transitions contains time diversity. A similar conclusion is made in [13] with regard to the Rician channel. In our case, we find the best four-state code depends on the fading bandwidth and on E_b/N_o where E_b is the unfaded, energy per bit and $N_o/2$ is the spectral height of the white Gaussian noise. In our studies, we use the Viterbi algorithm with the minimum distance metric to decode the trellis coded modulation symbols. This metric is optimum for the Gaussian channel, but not for fading channels. However, this metric is easily implemented. We do not use amplitude channel state information in our metric as it was found through simulation to yield a small performance improvement.

III. Perfect Coherent Detection

The phasor A_i in (1) has both an amplitude and phase. Also there is a carrier offset phase associated with the transmitted signal which is not shown in (1). In this section, results are presented when these two phases are ideally removed, thus leaving only the phase due to the modulation. Then the amplitude is the only faded element. In Figs. 3, 4, and 5, we present our simulation results on the average bit error probability as a function of unfaded, $2E_b/N_o$ for the light shadowing model. Three values of fading bandwidth are considered and, as one would expect, the results get better as the fading bandwidth increases; that is, as the channel becomes more random and better suits the coding technique employed. As shown in [11], there is a direct relation between increased fading bandwidth and interleaving code symbols in the transmitter and deinterleaving them before decoding. For instance, performance results for a higher fading bandwidth are equivalent to those when the actual fading bandwidth is lower and interleaving is utilized. Interleaving attempts to combat channel memory by producing an effective increase in channel fading bandwidth. When interleaving is used the interleaver is placed between the trellis encoder and the PSK

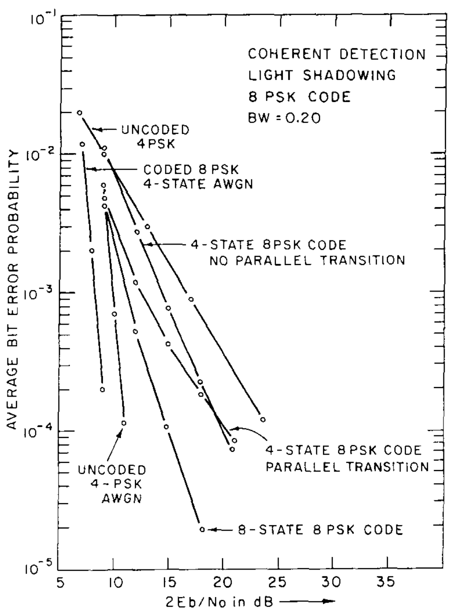

Fig. 4. Average bit error probability for the codes from Fig. 2 for a (normalized) fading bandwidth of 0.20 and a light shadowing fading model.

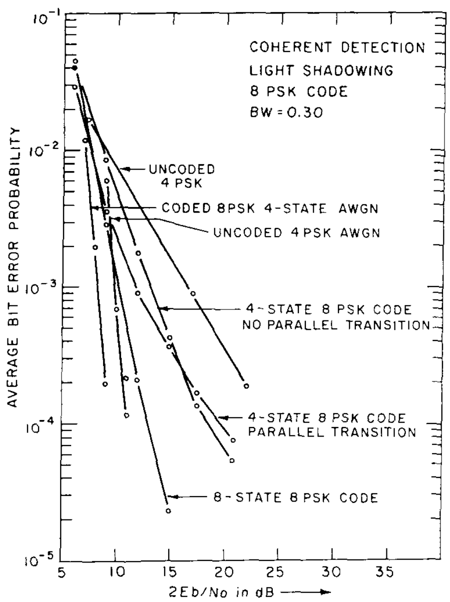

Fig. 5. Average bit error probability for the codes from Fig. 2 for a (normalized) fading bandwidth of 0.30 and a light shadowing fading model.

modulator shown in Fig. 1. The trellis decoder there will then consist of the tandem connection of a demodulator, a deinterleaver and a Viterbi decoder.

All codes given in Fig. 2 are considered in Figs. 3–5. Clearly the eight-state code gives the best performance. For four-state codes and speech error rates, i.e., $P_b = 10^{-3}$, Ungerboeck's four-state code [see Fig. 2(a)] is optimum. For lower error rates the code from [12] and [13] [see Fig. 2(b)] is optimum as long as the fading bandwidth is large enough. A simulation of the fast fading, Rayleigh channel, a special case of our model, showed four-state code performance, with and without parallel transitions, to be about the same for a fading

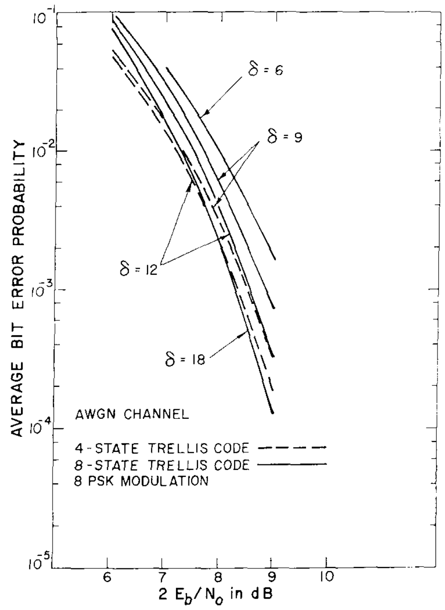

Fig. 6. Decision depth sensitivity four- and eight-state, 8 PSK codes: AWGN channel.

bandwidth of 0.10 and $P_b = 10^{-3}$. For lower P_b, the four-state code without parallel transitions was clearly best. Similar results would be expected for the Rician channel. Thus, code optimality for speech error rates depends on the presence of the shadowing phenomenon.

The number of trials used in our simulations was such that the relative change in the average bit error probability was 10 percent or less as this number was increased. Typically, a million symbols, i.e., two million information bits, were used to determine the bit error probability.

An important consideration in digital speech transmission is the time delay. In our satellite application, this delay is composed of a propagation delay of 250 ms plus the delay in producing the receiver output speech waveform. Most of the latter delay is composed of the decoding delay plus the delay due to interleaving. The larger the interleaving depth, the better the protection against long duration fades. However, this leads to a large time delay due to interleaving. To permit the interleaving depth to be as large as possible one should use as small a decoding delay δ as possible. For the AWGN channel, Ungerboeck recommends using four times the code constraint length. For the four-state codes this gives $\delta = 12$ symbols and for the eight-state codes we have $\delta = 18$ symbols. This figure was used for the results in Figs. 3–5. In Fig. 6, we demonstrate the sensitivity of P_b to perturbation in δ for the AWGN channel. In Fig. 7, we do the same for the light shadowing channel. Clearly, the latter case indicated less sensitivity of P_b to δ than the former. This is fortunate because using smaller δ in fading applications will result in the possible *use of larger interleaving depth and thus improved protection against slow fades.*

IV. 8 DPSK Trellis Codes

In [8], the sensitivity of P_b to phase jitter was investigated. This was done by attenuating the phase jitter due to the angle of $\mathcal{L}[\{A_i\}]$ in (1) rather than removing it entirely as in Section III. For light shadowing a maximum rms phase jitter of 4.5° could be tolerated before 1 dB of fade margin was lost at $P_b = 10^{-3}$. The fade margin is the increase in E_b/N_0 that is needed to achieve a given value of P_b for a fading condition relative to the same P_b for the AWGN channel.

Some first-order statistics of the phase jitter for our fading

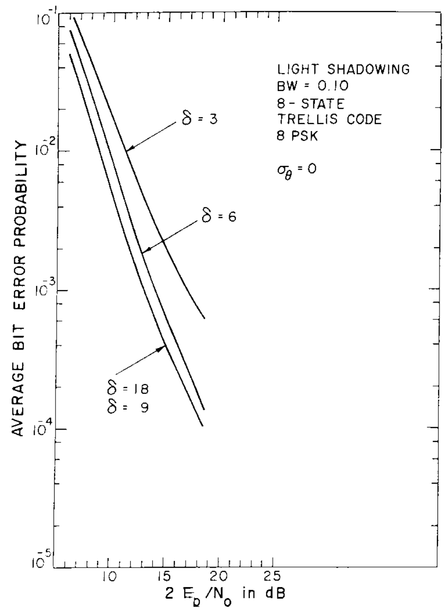

Fig. 7. Decision depth sensitivity for light shadowing: eight-state code. σ_θ is the rms phase jitter due to fading.

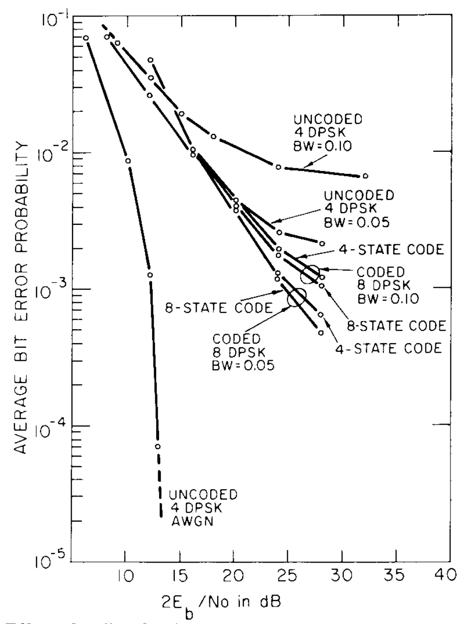

Fig. 8. Effect of coding for the average shadowing model, for $BW = 0.5$ and $BW = 0.10$. The modulation is DPSK.

TABLE II
ABSOLUTE AND DIFFERENTIAL RMS PHASE JITTER FOR LIGHT AND AVERAGE SHADOWING

Differential Phase Standard Deviation in Degrees	Fading Model	
	Shadowing	Bandwidth
3.15	Light	0.025
4.70	Average	0.025
4.70	Light	0.05
6.88	Average	0.05
7.45	Light	0.10
10.31	Average	0.10
12.60	Light	0.20
16.67	Average	0.20

Absolute Phase Standard Deviation in Degrees	Fading Model	
	Shadowing	Bandwidth
22.77	Light	NA
27.3	Average	NA

model are shown in Table II. It is clear that differential phase jitter between successive symbol samples can be quite low, especially for low fading bandwidth. Thus, the performance of the eight-state code in Fig. 2 but with differential 8 PSK modulation was determined. In this case, the Viterbi decoder input is $R_i R_{i-1}^*$ where R_i^* is the complex conjugate of R_i, which yields the signal term $A_i A_{i-1}^* e^{j(\phi_i - \phi_{i-1})}$ where $\phi_i - \phi_{i-1}$ is the trellis coded phase, as ϕ_i was initially differentially encoded. The Viterbi decoding algorithm was used as before and a minimum distance metric was used. This is not the optimum metric and further improvement may be possible over what is presented herein. Recall that [11] earlier reported on use of DPSK modulation with conventional codes. As well, [8] and [9] consider the performance of trellis coded DPSK modulation on fading channels.

Our results for the average shadowing condition is shown in

TABLE III
FADE MARGINS AND CODING GAINS AT A BIT ERROR PROBABILITY OF 10^{-3} FOR 4 DPSK AND 8 DPSK TRELLIS CODED MODULATIONS WITH "AVERAGE" SHADOWING FADING MODEL. THE FOUR- AND EIGHT-STATE CODES ARE FROM [6]

Modulation	Code States	BW	Fade Margin dB	Coding Gain dB
Uncoded 4 DPSK	NA	0.10	∞	NA
Coded 8 DPSK	4	0.10	18.0	∞
Coded 8 DPSK	8	0.10	17.0	∞
Uncoded 4 DPSK	NA	0.05	30.0	NA
Coded 8 DPSK	4	0.05	13.0	17.0
Coded 8 DPSK	8	0.05	12.0	18.0

Fig. 8. One notes that increased fading bandwidth does not lead to improved performance due to an increase in differential phase jitter (see Table II). The fade margins are tabulated in Table III. One notes that due to phase jitter uncoded 4 DPSK cannot satisfy a $P_b = 10^{-3}$ requirement. A 12 dB fade margin is acceptable in the Canadian MSAT system at this error probability. For the coded case this is met for a fading bandwidth of 0.05 but not for 0.10. The former fading bandwidth is approximately that observed by a vehicle traveling at 60 mph for a 800 mHz frequency allocation, whereas the latter is bandwidth for an L-band system (i.e., a frequency allocation of 1.5 GHz). This is for a symbol rate of 1200 symbols/s. Thus, eight-state DPSK trellis coded modulation meets the required fade margin for the 800 MHz system but not for the L-band system.

At lower speeds, and thus decreased fading bandwidth, one needs interleaved transmission. We investigated this in the following approximate manner. Assume the fading bandwidth was 0.025 and the interleaving depth was eight. The channel simulation was then carried out at the larger fading bandwidth of 0.20, or at eight times 0.025, and the rms phase jitter was reduced through attenuation to its value for a bandwidth of 0.025. Note that the reduced phase jitter still varies in time according to the larger fading bandwidth, 0.20, but its rms

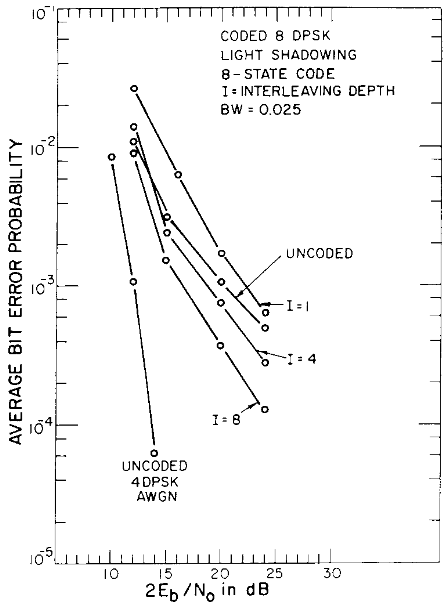

Fig. 9. Effect of interleaving on coded 8 DPSK performance for light shadowing and $BW = 0.025$.

value is set to correspond to a fading bandwidth of 0.025. Thus, in practice, P_b will probably be better than that provided by this method as the true phase variation in time is slower. Our simulation results are shown in Fig. 9. Clearly, interleaving is very effective in compensating for slow fades. In reality, slow fades are not a problem and attention in the future should be concentrated on compensating for the (fast) phase jitter that occurs in the L-band application. Higher dimensional, trellis coded 8 DPSK modulation may yield the required fade margin in this case.

As a further point we found the best four-state trellis code from Fig. 2 for speech error rates for DPSK modulation. For the light and average shadowing model cases considered in Fig. 8, the code with parallel transitions in Fig. 2 outperformed the code without them. The same result was found for the case with interleaving given in Fig. 9. For DPSK modulation the code with parallel transitions was 2 dB better than the code without them at $P_b = 10^{-3}$. This gain is 0.5 dB more than occurred for PSK modulation with perfect coherence. Finally, we checked performance of most codes for a first-order Butterworth fading spectrum. This case gave more coding gain relative to the third-order Butterworth fading spectrum considered earlier. This is because the lower order filter presents less attenuation to high frequency fades and thus represents a more random channel.

References

[1] D. Divsalar and M. K. Simon, "Trellis coded modulation for 4800 to 9600 bps transmission over a fading satellite channel," *JPL Pub.*, vol. 86-8, June 1, 1986, Pasadena, CA; also, *IEEE J. Select. Areas Commun.*, vol. SAC-5, pp. 162–175, Feb. 1987.

[2] C. Loo, "A statistical model for a land mobile satellite link," in *Links for the Future (ICC'84), Science, Systems, and Services for Communication*, P. Dewilde and C. A. May, Ed. New York: IEEE/Elsevier, North-Holland, 1984.

[3] C. Loo, "Measurements and models of a mobile-satellite link with applications," presented at Proc. GLOBECOM'85, New Orleans, LA, Dec. 2–5, 1985.

[4] ——, "A statistical model for a land mobile satellite link," *IEEE Trans. Vehic. Technol.*, vol. VT-34, pp. 122–127, Aug. 1985.

[5] C. Loo, E. E. Matt, J. S. Butterworth, and M. Dufour, "Measurements and modelling of land-mobile satellite signal statistics," presented at 1986 Vehic. Technol. Conf., Dallas, TX, May 20–22, 1986.

[6] G. Ungerboeck, "Channel coding with multilevel/phase signals," *IEEE Trans. Inform. Theory*, vol. IT-28, pp. 55–67, Jan. 1982.

[7] P. J. McLane, P. H. Wittke, and P. K-M. Ho, "A study on combined channel coding and modulation for mobile satellite communications," Dept. Elec. Eng., Queen's University, Kingston, Ont., Canada, Final Rep., DSS Contract OST85-00197.

[8] P. J. McLane, P. H. Wittke, P. K.-M. Ho, and C. Loo, "PSK and DPSK trellis codes for fast fading, shadowed mobile satellite communication channels," in *Proc. 1987 Int. Conf. Commun.*, Seattle, WA, June 7–10, 1987, pp. 21.1.1–21.1.6.

[9] M. K. Simon and D. Divsalar, "The performance of trellis coded multilevel DPSK on a fading mobile satellite channel," in *Proc. 1987 Int. Conf. Commun.*, Seattle, WA, June 7–10, 1987, pp. 21.2.1–21.1.7.

[10] J. W. Modestino and S-Y. Mui, "Convolutional code performance in the Rician fading channel," *IEEE Trans. Commun.*, vol. COM-24, pp. 592–606, June 1976.

[11] S.-Y. Mui and J. W. Modestino, "Performance of DPSK with convolutional encoding on time-varying fading channels," *IEEE Trans. Commun.*, vol. COM-25, pp. 1075–1083, Oct. 1977.

[12] S. G. Wilson and Y. S. Leung, "Trellis-coded phase modulation on Rayleigh channels," in *Proc. 1987 Int. Conf. Commun.*, Seattle, WA, June 7–10, 1987, pp. 21.3.1–21.3.5.

[13] M. K. Simon and D. Divsalar, "Multiple trellis coded modulation (MTCM) performance on a fading mobile satellite channel," in *Proc. 1987 GLOBECOM*, Tokyo, Japan, Nov. 15–18, 1987, pp. 43.8.1–43.8.6.

Asymptotic Performance of *M*-ary Orthogonal Modulation in Generalized Fading Channels

P. J. CREPEAU

Abstract—**The asymptotic ($M \to \infty$) probability of symbol error $P_{e,m}$ for M-ary orthogonal modulation in a Nakagami-m fading channel is is given by the incomplete gamma function $P(m, mx)$ where $x = \ln 2/(E_b/N_o)$ and E_b is the average energy per bit. For large signal-to-noise ratio this leads to a channel where the probability of symbol error varies as the inverse mth power of E_b/N_o. These channels exist for all $m \geq 1/2$. The special case of $m = 1$ corresponds to Rayleigh fading, an inverse linear channel.**

I. Introduction

It is well known [1], [2] that the theoretical performance of M-ary orthogonal modulation in additive white Gaussian noise is given asymptotically for large alphabet size M by

$$\lim_{M\to\infty} P_e\left(\frac{E_b}{N_0}, M\right) = \begin{cases} 1, & E_b/N_0 < \ln 2 \\ 0, & E_b/N_0 > \ln 2 \end{cases} \quad (1)$$

where P_e is the probability of symbol error, E_b is the energy per bit, and N_o is the one-sided noise power spectral density. This result is valid for both coherent and noncoherent channels. Recently, the corresponding asymptotic result for M-ary orthogonal modulation in a slow nonselective Rayleigh

Paper approved by the Editor for Coding Theory and Applications of the IEEE Communications Society. Manuscript received September 22, 1987; revised February 9, 1988. This work was supported by the Space and Naval Warfare Systems Command.

The author is with the Information Technology Division, Naval Research Laboratory, Washington, DC 20375.

IEEE Log Number 8823620.